ADVANCED FUNCTIONAL MATERIALS
www.afm-journal.de

Engineering Natural Pollen Grains as Multifunctional 3D Printing Materials

Shengyang Chen, Qian Shi, Taesik Jang, Mohammed Shahrudin Bin Ibrahim, Jingyu Deng, Gaia Ferracci, Wen See Tan, Nam-Joon Cho, and Juha Song**

The development of multifunctional 3D printing materials from sustainable natural resources is a high priority in additive manufacturing. Using an eco-friendly method to transform hard pollen grains into stimulus-responsive microgel particles, we engineered a pollen-derived microgel suspension that can serve as a functional reinforcement for composite hydrogel inks and as a supporting matrix for versatile freeform 3D printing systems. The pollen microgel particles enabled the printing of composite inks and improved the mechanical and physiological stabilities of alginate and hyaluronic acid hydrogel scaffolds for 3D cell culture applications. Moreover, the particles endowed the inks with stimulus-responsive controlled release properties. The suitability of the pollen microgel suspension as a supporting matrix for freeform 3D printing of alginate and silicone rubber inks was demonstrated and optimized by tuning the rheological properties of the microgel. Compared with other classes of natural materials, pollen grains have several compelling features, including natural abundance, renewability, affordability, processing ease, monodispersity, and tunable rheological features, which make them attractive candidates to engineer advanced materials for 3D printing applications.

1. Introduction

Additive manufacturing has become a powerful and versatile strategy for the fabrication of advanced materials.[1] 3D printing enables product fabrication without the need for molding or tooling, which increases the freedom of part design and enables the sustainable and cost-effective construction of objects with complex geometries.[2] Moreover, the cost of adjusting the 3D model is minimal, which is beneficial for mass customization.[1] Various additive manufacturing technologies have been developed for different material types, such as selective lasering melting and electron beam melting for metal 3D printing,[3] selective laser sintering and digital light processing for ceramics,[4] and fused deposition modeling, stereolithography, and 3D plotting for polymers.[5]

Among the 3D printing techniques, direct ink writing (DIW) has the most significant potential for biomedical applications because it enables the incorporation of live cells.[6] The ideal ink for DIW printing should possess suitable viscoplastic properties for nozzle extrusion and self-supporting properties to maintain structural integrity after deposition.[7] Among the potential inks for DIW printing, hydrogels have been widely used for various biomedical products, including tissue scaffolds, because they can mimic most biological soft tissues.[8] 3D-printed hydrogel scaffolds provide appropriate conditions for cell attachment and development, as their customizable 3D networks provide sufficient space for cell clusters, facilitating the circulation of essential metabolites and nutrients for the encapsulated or attached cells.[8a,9] However, hydrogels are characterized by low mechanical and physiological stability and bioinertness.[8a] Thus, composite hydrogel systems have been proposed to provide functions and properties not attainable by any single hydrogel. These composites are formed by mixing, immobilizing, or hybridizing single hydrogels with a diverse range of reinforcements in the forms of particles, anisotropic fillers, and fibers.[8–10] These reinforcements significantly alter the rheological properties of the hydrogel inks, which may improve the printability of the composite hydrogels up to a certain loading amount.[11] For instance, nano-platelets[12] and nano-fibers[13] have been found to endow hydrogel bioinks with solid-like jamming behavior, which helps complex 3D structures to hold together in air environments. The main drawback of current hydrogel composite inks is nozzle clogging, which is a more significant issue in inks with higher reinforcement loading content.

Supporting matrices have been introduced to extrusion-based 3D printing systems to solve the problem of soft matter printability.[14] An advanced technique called freeform 3D printing enables the omnidirectional deposition of ink materials, such as hydrogels,[15] cells,[16] and silicone rubber,[17] within a supporting

S. Chen, Q. Shi, W. S. Tan, J. Song
School of Chemical and Biological Engineering
Nanyang Technological University
Singapore 637459, Singapore
E-mail: songjuha@ntu.edu.sg
T. Jang
Department of Materials Science and Engineering
Chosun University
Gwangju 61452, Republic of Korea
M. S. B. Ibrahim, J. Deng, G. Ferracci, N.-J. Cho
School of Materials Science and Engineering
Nanyang Technological University
Singapore 639798, Singapore
E-mail: njcho@ntu.edu.sg
The ORCID identification number(s) for the author(s) of this article can be found under https://doi.org/10.1002/adfm.202106276.

DOI: 10.1002/adfm.202106276

matrix. The embedded ink can preserve the printed 3D structure before it is fully cured, making slow curing applicable to 3D printing. To realize freeform 3D printing, the supporting matrix material needs to meet several criteria: i) its rheological properties should complement those of the ink; ii) it should be chemically and structurally stable; and iii) it should be recyclable for multiple printing cycles.[14,18] Numerous supporting matrix systems, including Carbopol granular gel medium,[15a] gelatin slurry support bath,[15b] and Laponite nanoclay suspension,[19] have been developed to accomplish the 3D printing of various inks. The materials used for developing hydrogel composites and supporting matrices are distinct, and identifying a naturally available, abundant, and renewable material template that requires minimal processing will be beneficial for the 3D printing industry.

Herein, we report the development of a pollen-derived microgel suspension that is readily prepared from abundant renewable pollen grains and can be easily tuned via a single step to create advanced materials that are useful as functional reinforcements for composite hydrogel bioink systems and as freeform 3D printing supporting matrices (**Figure 1**). This approach builds on our recent efforts to mechanically transform hard pollen grains into soft, stimulus-responsive microgel particles.[20] Each pollinating plant species renewably produces an abundant supply of pollen grains, which occur as monodisperse, hollow microcapsules with unique ornamental features depending on the particular species. Compared to biomaterial-based gels, produced by bottom-up synthesis methods with biomolecules,[21] pollen microgels are more advantageous for 3D printing systems, which often require a large volume of materials with good structural uniformity, consistent and tunable rheological behavior, and high cost-efficiency and scalability besides excellent sustainability of material sources. Particularly, pollen microgels can provide structural stability and stimulus-responsive drug delivery capabilities of the printed structures as an ink material. The mechanically strong exine layer provides good structural support to the printed structure, while the inflatable smart intine layer modulates drug release in the existence of environmental stimulus. As a supporting matrix, the pollen microgel suspension is highly advantageous since pollen grains are an abundant and affordable starting material with a uniform size distribution, tunable and consistent rheological behavior.

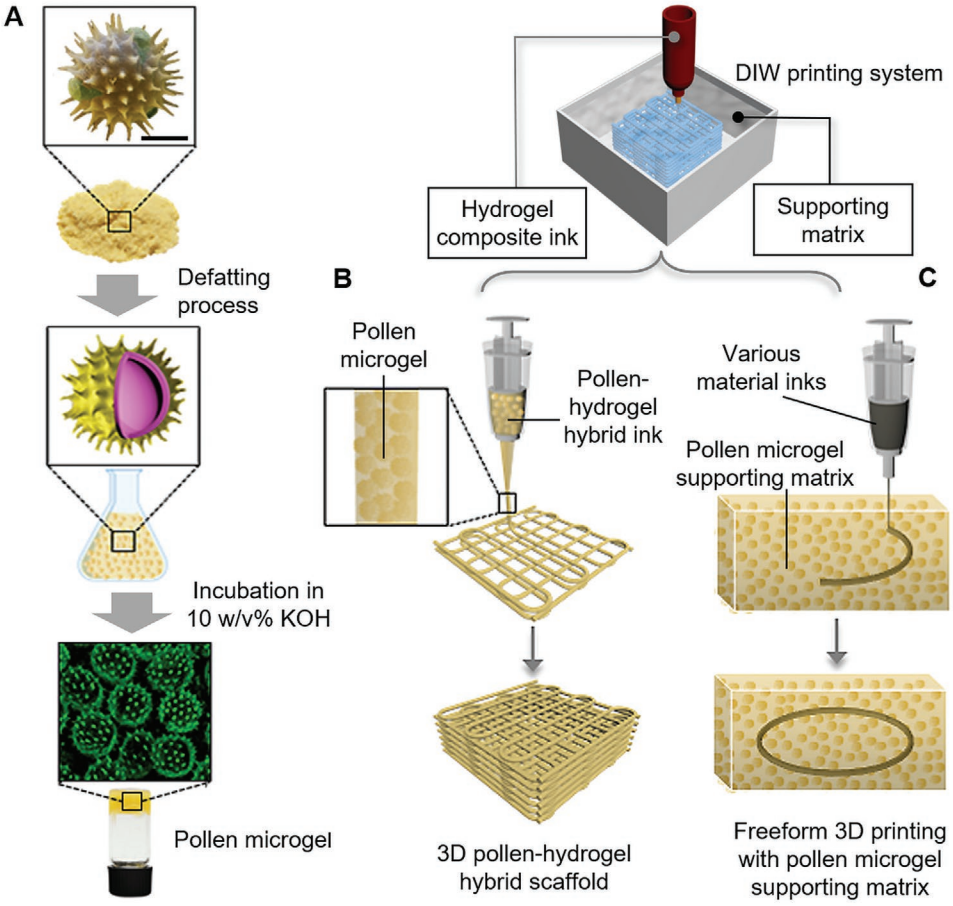

Figure 1. Illustration of pollen microgel as a bioink and supporting matrix material for 3D printing applications. A) Process of microgel fabrication from natural pollen grains. Pollen grain incubation in alkaline solution to yield microgel with tunable rheological properties. The scale bar represents 10 µm. DIW printing system with hydrogel-based inks and with or without a supporting matrix, where B) the pollen microgels can be combined with hydrogel materials to form hybrid materials that can serve as biocompatible inks with new functionalities, such as controlled release; and C) pollen microgel medium acting as a supporting matrix for freeform 3D printing using a wide range of inks.

In this study, using a method akin to soapmaking, sunflower pollen was readily transformed into monodisperse, hollow microgel particles, and a microgel suspension was formed (Figure 1A). As illustrated in Figure 1B,C, we used the pollen-derived microgel particles to develop pollen-derived 3D printing materials that were: i) assembled with hydrogels such as alginate and hyaluronic acid (HAc) to create 3D-printed functional scaffolds for cell culture applications (Figure 1B); and ii) utilized as a supporting matrix for the freeform 3D printing of alginate and silicone rubber inks (Figure 1C). The pollen microgels present in the composite hydrogel inks were investigated to characterize their rheological behavior in the inks and stimulus-responsive smart properties in the hydrogel matrix. Moreover, the feasibility of the pollen microgel-based granular medium as a supporting matrix for 3D printing was demonstrated through rheological tests and proof-of-concept 3D printing products.

2. Results and Discussion

2.1. Preparation of Pollen-Incorporated Hydrogel Hybrid Inks for 3D Printing

When building 3D architectures using pollen microgel building blocks, an adhesive matrix material will make the microgels more suitable for 3D printing. We selected alginate, which is one of the most common hydrogel inks used in various 3D printing systems owing to its simple and cell-friendly crosslinking process, and formed pollen microgel–hydrogel hybrid inks. Considering that nano or micro-sized particles affect the rheological behavior of alginate ink,[22] we first characterized the rheological behavior and corresponding printability of the pollen–alginate hydrogel inks as a function of the pollen microgel fraction.

We tested the rheological properties of pollen microgels before and after KOH treatment (**Figure 2**A). First, 10 vol% of pollen microparticles were dispersed in water. The viscosity of the defatted pollen grains was two orders of magnitude larger than that of 10 v/v% KOH-treated pollen owing to particle jamming in the defatted grains. However, once the pollen grains were transformed into microgels through alkali treatment, the pollen-dispersed solutions had almost identical rheological behaviors, irrespective of the KOH treatment duration. The viscosity of pollen microgel suspension was governed by the volume fraction and gel stiffness of pollen microgels.[23] Under the fixed volume fraction, the higher stiffness of the defatted pollen grains led to higher viscosity compared with softer pollen microgels. This finding is consistent with the softened exine layer of pollen microgels, which allows for the easy compression of the microgels to avoid particle jamming under shear and thus enables a free-flowing solution.[24] Moreover, spiky appendages on the surface of pollen microgels minimize the contact between microgels, reducing aggregation among microgels, thus improving the structural stability of pollen microgels in the fluid. Pollen microgels treated with KOH for 6 h were chosen owing to their good swelling capability and structural integrity.[20]

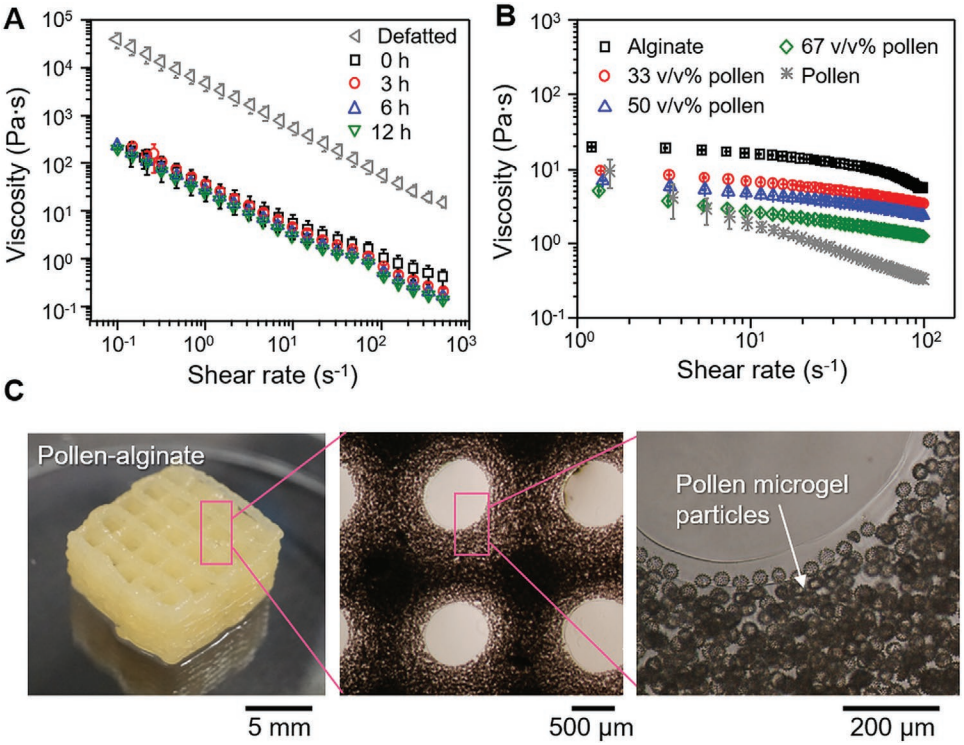

Figure 2. Pollen microgel–alginate hydrogel hybrid 3D printing ink for printability. A) Viscosity as a function of shear rate under different pollen microgel processing times (0, 3, 6, or 12 h). B) Viscosity as a function of shear rate for pollen–alginate hybrids with different alginate-to-pollen volume ratios: 1:0 (alginate), 1:2 (33 v/v% pollen), 1:1 (50 v/v% pollen), 2:1 (67 v/v% pollen), 0:1 (pollen). C) Optical images of pollen–alginate scaffold crosslinked and freeform-3D-printed in gelatin supporting matrix.

Furthermore, various pollen–alginate composite inks with volumetric ratios of 0:1, 1:2, 1:1, 2:1, and 1:0 were prepared to optimize the printing ink viscosity (Figure 2B). All pollen–alginate hybrid inks exhibited a lower viscosity than the pure alginate ink because of dilution by the high water content from the swollen pollen microgels. All prepared inks could be extruded without jamming or clogging regardless of the volume fraction of the pollen microgels. The single-layer structures printed with various pollen–alginate inks were solidified after post-treatment using 153 mM $CaCl_2$ solution (Figures S1 and S2, Supporting Information). The pollen microgels were well distributed within the alginate matrix without any particle aggregation, unlike typical polymer–particle composite systems.[25] However, the self-supportability of pollen–alginate inks was still suboptimal, which led us to further improve the platform design.

More specifically, multilayer 3D structures were fabricated through freeform 3D printing in gelatin slurry with $CaCl_2$ (Figure 2C and Figure S3, Supporting Information). Using the supporting matrix, 3D scaffolds with good structural stability could be fabricated. However, when the pollen fraction in the pollen–alginate inks was >67%, the pollen microgel connectivity was not sufficient to maintain structural integrity once the printed structures were removed from the supporting matrix. Thus, pollen–alginate inks with a volumetric ratio of 1:1 were used for fabricating the 3D pollen–alginate scaffolds. Moreover, compared with previously reported microgel 3D printing systems,[21b,c,26] the pollen microgels possessed a smaller size (<50 µm) with uniform size distribution. Thus, a consistent microstructure was achieved within the composite hydrogels, improving the reproducibility of the printed product.

2.2. Functional Hydrogel Scaffolds with Smart Pollen Microgels

Pollen microgels are plant-derived smart materials that are responsive to solution pH and ethylenediaminetetraacetic acid (EDTA).[20] Thus, they can be used as smart drug carriers for composite hydrogel scaffolds. For the freeform 3D printing experiments, we chose photocurable glycidyl methacrylate hyaluronic acid (GM-HAc)-alginate hydrogels with an HAc-to-alginate weight ratio of 8:1.[27] Alginate was introduced to stabilize printed pollen–hydrogel inks by physical crosslinking in the Ca^{2+}-rich gelatin matrix. It can be removed through EDTA treatment after the second hydrogel GM-HAc is crosslinked during the post-curing process. Moreover, drug-loaded pollen microgels have been found to undergo additional deswelling with excessive Ca^{2+} during the physical crosslinking of alginate.[20] In the current study, the 3D pollen–hydrogel scaffolds were successfully obtained after the post-curing process (**Figure 3**A). For a proof-of-concept drug delivery study, we chose a hydrophilic fluorescent dye, rhodamine B (RhB), as a tracer dye. Given that this dye is a relatively small molecule with good diffusion, in the

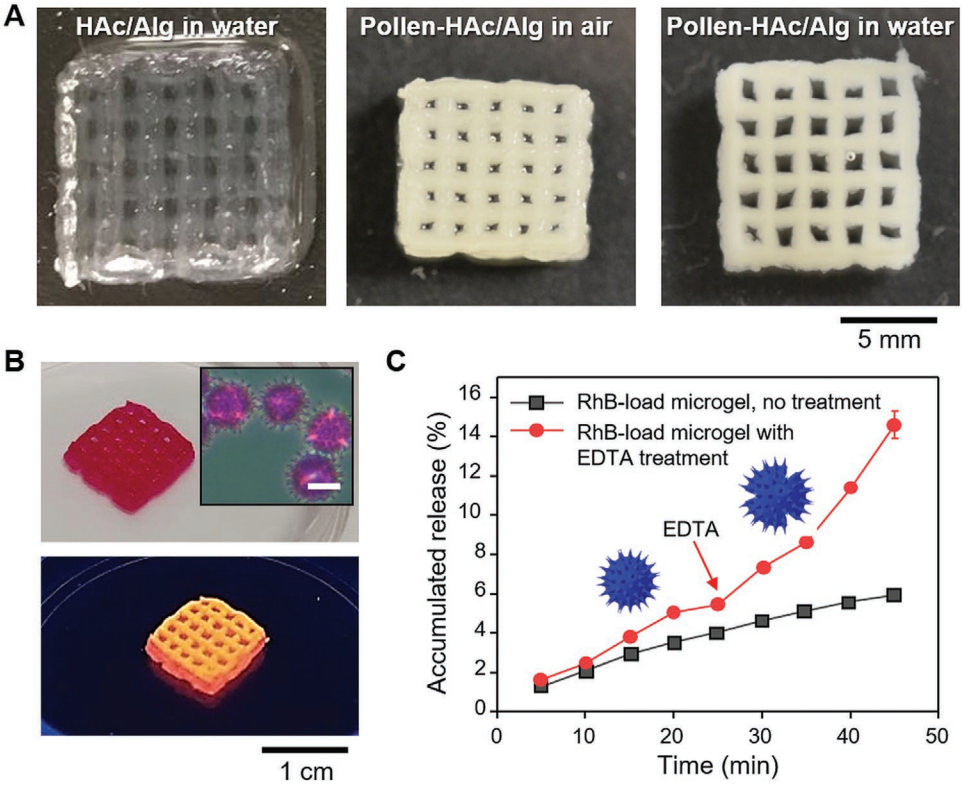

Figure 3. 3D-printed pollen microgel–hydrogel scaffolds for drug loading and release. A) Optical images of hyaluronic acid (HAc)/alginate (Alg) scaffolds printed in gelatin supporting matrix with or without pollen microgels. All scaffolds were post-cured under UV irradiation after printing. B) Optical images of a Rhodamine B (RhB)-loaded pollen–HAc/Alg hybrid scaffold printed and crosslinked under UV irradiation. The inset displays RhB-loaded pollen microgels. The scale bar represents 10 µm. C) Dye release of RhB-loaded pollen microgels mimicking drug release. Accumulated release as a function of time.

absence of EDTA treatment, it can passively diffuse through the nanoporous channels of the pollen exine layer (Figure S4, Supporting Information). Thus, the fabricated hydrogel scaffold with RhB-loaded pollen microgels exhibited the inherent red color of RhB (Figure 3B). Moreover, the amount of RhB released through the pollen microgel exine layer linearly increased over time (Figure 3C). However, upon EDTA treatment, the released amount and rate of release appreciably increased with time owing to the aperture openings in the pollen microgels.[20] Therefore, the stimulus-responsive release behavior of drugs loaded onto the pollen microgels can be tuned and optimized by minimizing the uncontrolled release caused by passive diffusion, which can be achieved by selectively covering the nanopores in the exine layer with an additional coating layer.[28] Mundargi et al.,[29] reported the prolonged-release behavior of drug-loaded sunflower pollen grains after being coated with a thin alginate layer even under the existence of stimuli. Therefore, the additional coating layer, which can cover and block nanopores on the shell, allows the drug release to be initiated only by the aperture opening of microgels with the existence of stimuli.

2.3. Pollen–Hydrogel Scaffolds for 3D Cell Culture Platforms

The 3D-printed pollen–hydrogel scaffolds could also be an excellent platform for 3D cell culture owing to the excellent biocompatibility of pollen[30] and improved mechanical stability of the composite hydrogels.[5,10b] Owing to its ≈50% lower swelling ratio than that of the pure hydrogel, the swollen pollen–hydrogel scaffold exhibited better structural stability in the culture medium (cf. Figure 3A). Furthermore, we assessed the pollen–HAc/Alg scaffold as a substitute for inverted colloidal crystal (ICC) hydrogels, which are widely utilized for 3D cell culture platforms despite their time-consuming and laborious fabrication.[31] Particularly, ICC scaffolds are commonly used to form multicellular spheroids with liver cells as a 3D in vitro testbed of liver functions. However, the fabrication of ICC scaffolds is laborious, time-consuming with a multi-step process.[32]

To construct uniform, highly interconnected pores within the 3D-printed scaffolds, we designed a five-layer scaffold for culturing 3D cell aggregates, where the continuous printing path formed a pattern with holes shaped like isosceles right triangles (Figure S5, Supporting Information). The first, third, and fifth layers had small triangular holes (1 cm leg length) for cell transportation, while the second and fourth layers had larger triangular holes (2 cm leg length) for storing cell aggregates. Based on this design, the 3D scaffold was successfully printed with the pollen–HAc/alginate hybrid ink in 12 min at a feed rate of 1.5 mm s^{-1} (**Figure 4**A). The filament diameter was ≈250 μm, which made the actual leg length of the small triangle hole ≈500 μm (Figure 4B). Given the highly interconnected porous structure of the 3D-printed pollen–HAc/alginate hydrogels, we compared the performances of these scaffolds with those of poly(ethylene glycol)-diacrylate (PEGDA) ICC hydrogels. Because of the hierarchical scaffold structure, the Huh-7.5 liver cell line was chosen for in vitro cell studies. To provide cells with anchoring points, both 3D-printed pollen–HAc/alginate hydrogels and PEGDA ICCs were functionalized with type 1 collagen, one of the most abundant proteins in liver-derived extracellular matrices.[33]

Overall, the cells encapsulated in the 3D-printed pollen–HAc/alginate and the PEGDA ICC scaffolds were viable with good cell proliferation, indicating that both hydrogel scaffolds provided adequate exchange and diffusion of nutrients, oxygen, and metabolites to cells (Figure 4C,D). In all of the constructs, hepatocarcinoma cells were seeded as single cells with an efficiency exceeding 94%, although collagen-coated PEGDA ICCs achieved almost 100% cell seeding efficiency owing to the increased cell adhesion sites provided by the collagen coating (Table S1, Supporting Information). The highly interconnected and open porous structures of both 3D-printed pollen–HAc/alginate and PEGDA ICC hydrogels ensured cell infiltration throughout the construct (Figure 4C). The structures featured pronounced differences in cell morphology depending on the existence of the collagen coating layer. In particular, cells in the noncoated hydrogels formed clusters at the centers of the scaffold cavities owing to the lack of cell adhesion sites, whereas cells in the collagen-coated hydrogels were attached to the scaffold surface and formed clusters lining the wall cavities (Figure 4C,D and Figure S6, Supporting Information).

Moreover, owing to the 3D structural differences between the two types of scaffolds, cells in the PEGDA ICCs formed spherical aggregates, whereas cells in the 3D-printed pollen–HAc/alginate hydrogels formed irregularly shaped clusters of various sizes. Unlike the ICCs with uniform spherical pores, the triangular open holes of the 3D-printed pollen–HAc/alginate hydrogels allowed most cells to continuously grow in 3D without any shape-induced aggregation, even though small spherical clusters also occurred. More importantly, the pollen microgel autofluorescence could reveal the interfaces between cells and scaffolds without an additional scaffold-staining process.

2.4. Pollen Microgel Supporting Matrix for Freeform 3D Printing

Shear-thinning and viscoplastic supporting matrices have been introduced for omnidirectional freeform 3D printing using soft materials with a relatively slow solidification rate and poor self-supportability.[34] These supporting matrices have been formulated by mixing nanoparticles with polymer solutions or dispersing microgels in water or oil, and particularly, the rheological properties of microgel-based supporting matrices are affected by the microgel size, shape, and mechanical properties.[14,34a,b,35] Pollen microgels are naturally derived, readily-made, environmentally friendly, and sustainable potential materials for supporting matrices produced by freeform 3D printing because of their great abundance in nature, uniform size distribution, tunable mechanical properties through alkali treatment, and gel properties.

First, to validate the viscoplastic behavior of pollen microgel-based supporting matrices, shear stress was measured as a function of shear rate ($\dot{\gamma}$) (**Figure 5**A). All of the pollen microgel-based supporting matrices exhibited Bingham plastic behavior, showing good agreement with the Herschel–Bulkley (H–B) model ($\tau = \tau_0 + k\dot{\gamma}^n$) regardless of the KOH incubation time (0 to 9 h). By fitting the shear stress–shear rate curves using the H–B models, we determined three H–B parameters: the yield stress (τ_0), consistency index (k), and flow index (n). We also measured the stress-dependent storage

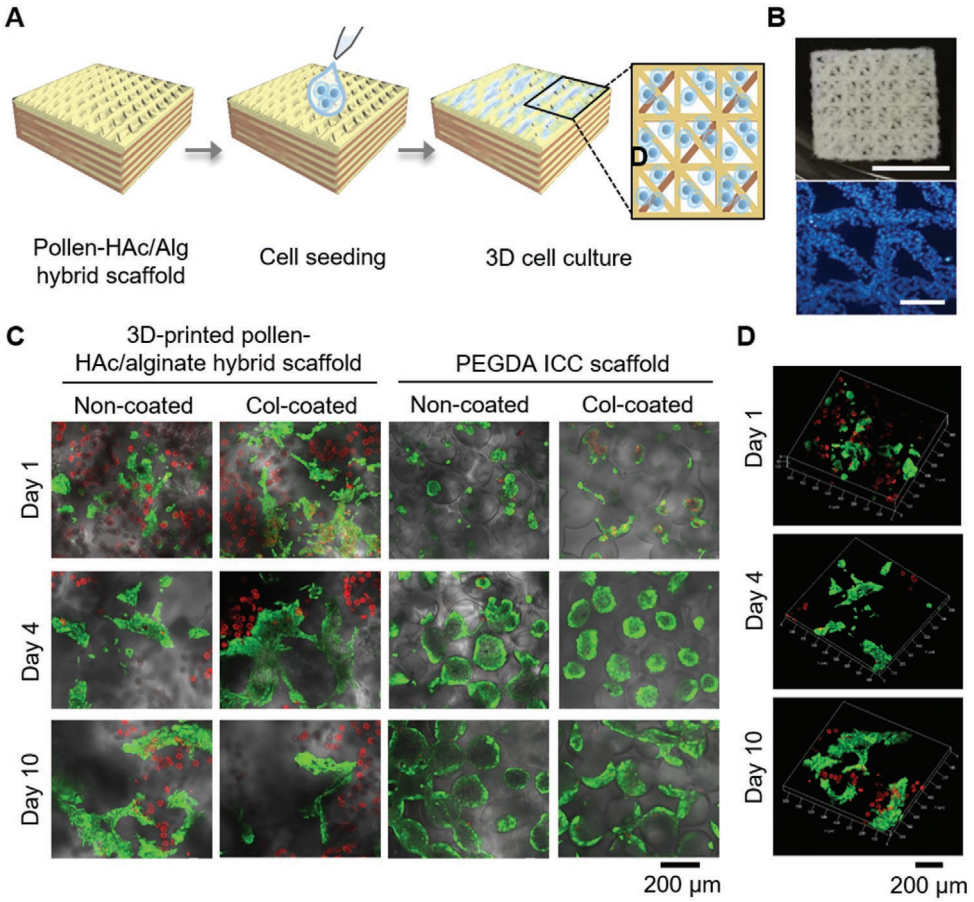

Figure 4. 3D cell culture scaffold based on pollen–HAc/alginate hybrid ink. A) Schematics of 3D cell culture on a pollen–HAc/alginate hybrid scaffold. B) Optical images of a 3D-printed pollen–HAc/alginate hybrid scaffold. The scale bars represent 5 mm (top) and 500 μm (bottom). C) Live/dead staining of Huh-7.5 cells cultured on a 3D-printed pollen–HAc/alginate hybrid scaffold (noncoated, Col-coated) compared with PEGDA ICCs (noncoated, Col-coated) on days 1, 4, and 10. Live cells were stained with calcein-AM, fluorescein green, whereas dead cells were stained with EthD-1, fluorescein red. Pollen particles presented red autofluorescence. D) 3D reconstructions of live/dead images of 3D-printed pollen–HAc/alginate scaffolds on days 1 (top), 4 (middle), and 10 (bottom).

and loss moduli from oscillatory shear rheometer tests and determined the yield stress, that is, the shear stress at which the storage modulus begins to decrease and the loss modulus begins to increase (Figure 5B). The yield stresses derived from both methods are summarized in **Table 1**. Additionally, the thixotropic behavior was assessed using a step test wherein structural breakdown and recovery were induced through stepwise programmed deformation (Figure 5C). We monitored three oscillatory intervals, applying three predetermined strain types: 1% strain ($\gamma < \gamma^{Y}$); 70% strain (breakdown, $\gamma > \gamma^{Y}$); and 1% strain (recovery, $\gamma < \gamma^{Y}$). The 95% recovery time and full recovery time were found to be 6 and 180 s, respectively, indicating that the pollen microgel-based supporting matrix featured excellent thixotropic behavior, comparable to that of a previously reported gellan fluid gel.[36] As the KOH incubation time increased, the pollen microgels became softer.[20] Thus, the storage and loss moduli of the pollen microgel media decreased as the alkali treatment continued. Finally, the rheological behavior of these pollen microgel-based supporting matrices was also affected by the volume fraction of microgels in water (Figure 5D). Therefore, pollen microgel-based supporting matrices can be tuned based on the KOH incubation time and volume fraction of pollen microgels in water; thus, for printing, the supporting matrices can be well matched with a corresponding ink material in terms of rheological behavior.

2.5. Pollen-Based Freeform 3D Printing Platform for Soft Matter

As a proof-of-concept study, freeform 3D printing was performed within the pollen microgel supporting matrix using two types of soft material inks: 7 wt% alginate and silicone rubber SE1700 with a base/catalyst/mineral oil ratio of 10:1:1.5.[17b] Both the shear-thinning alginate and silicone inks were printable, displaying dynamic viscosities of 10–100 Pa s at shear rates of 10–50 s^{-1}, a typical extrusion condition of 3D printing[37] (Figure S7, Supporting Information). Moreover, to enable freeform 3D printing, the yield stress and shear modulus of the viscoplastic silicone ink should be larger than those of the supporting matrix by at least one and two orders of magnitude, respectively.[35,38] Silicone inks have yield stresses of

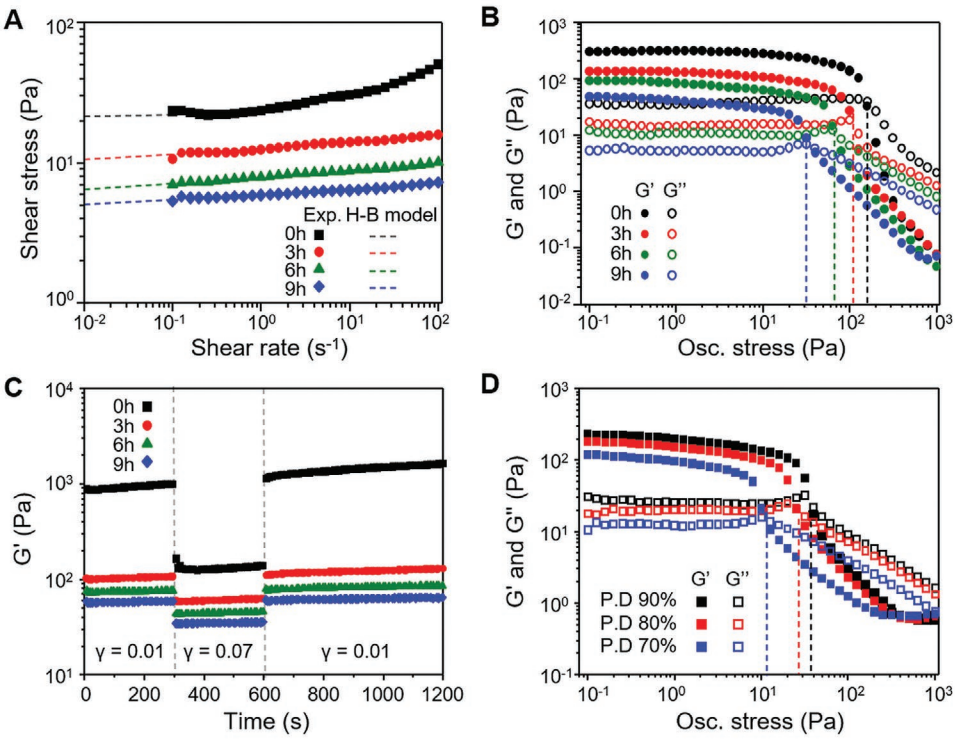

Figure 5. Optimizing the rheological properties of pollen microgels for use as a freeform 3D printing supporting matrix. A–C) Tuning of pollen microgel rheological properties based on the KOH incubation time. A) Shear stress as a function of shear rate for pollen microgels. Dashed lines depict the theoretical prediction of the Herschel–Bulkley model for a non-Newtonian fluid. B) Storage modulus (G′) and loss modulus (G″) as functions of oscillation stress at a frequency of 1 Hz for pollen microgel. Dashed lines represent the crossover points. C) Storage modulus (G′) and loss modulus (G″) as functions of time at a frequency of 1 Hz with different strain conditions (0–300 s: 1% strain; 300–600 s: 70% strain; 600–1200 s: 1% strain) for pollen microgel. D) Storage modulus (G′) and loss modulus (G″) as functions of oscillation stress at a frequency of 1 Hz for pollen microgels with different volume fractions (packing density PD = 90%, 80%, and 70%). Dashed lines represent the crossover points.

400–600 Pa and shear moduli of 10–20 kPa (Figure S7, Supporting Information).[17b] Thus, the optimal yield stress and shear modulus of the microgel-based supporting matrix should be ≈60 and ≈200 Pa, respectively. We chose a supporting matrix consisting of 6 h KOH-treated pollen microgels at 90% packing density (PD).

To demonstrate the supportability of the pollen microgel-based supporting matrix during 3D printing, complex printing paths were designed for the ink systems. During printing, writing the Chinese word 花粉 (English translation: pollen) requires multiple starting points and junctions for the total seventeen strokes of the two characters (**Figure 6**A, and Figure S8, Supporting Information). Each stroke had a 500 µm diameter and was drawn in a single pass, either intercepting or adjoining the pre-printed strokes at the optimal printing speed (Video S1, Supporting Information). The non-crosslinked alginate inks were stable during and after printing, as they were visible even after 3 h after the completion of printing. We also used polydimethylsiloxane (PDMS) ink made of SE1700, which required high-temperature curing at 50–80 °C.

To test the feasibility of the approach, a meshed dome frame was printed and subsequently cured at 75 °C for 24 h inside the pollen microgel (Figure S9, Supporting Information). The printed 3D dome structure was well solidified, maintaining its structural integrity without any significant deformation or collapse. To further prove the large-scale printing capability of the pollen-based freeform 3D platform, an actual-size 3D elbow mesh was designed and printed. The 3D printing path generation process has been reported in a previous paper[17b] (Figure S10, Supporting Information) and is described below:

Table 1. Yield stresses and storage moduli of various pollen microgel supporting matrix suspensions.

Pollen microgel supporting matrix	Steady shear rate sweep method	Dynamic oscillatory stress sweep method	
	Yield stress [Pa]	Yield stress [Pa]	G′ [Pa]
0 h KOH incubation	212.4	152.0	39.85
3 h KOH incubation	69.21	108.9	14.88
6 h KOH incubation	32.34	66.70	11.28
9 h KOH incubation	50.49	35.91	6.262

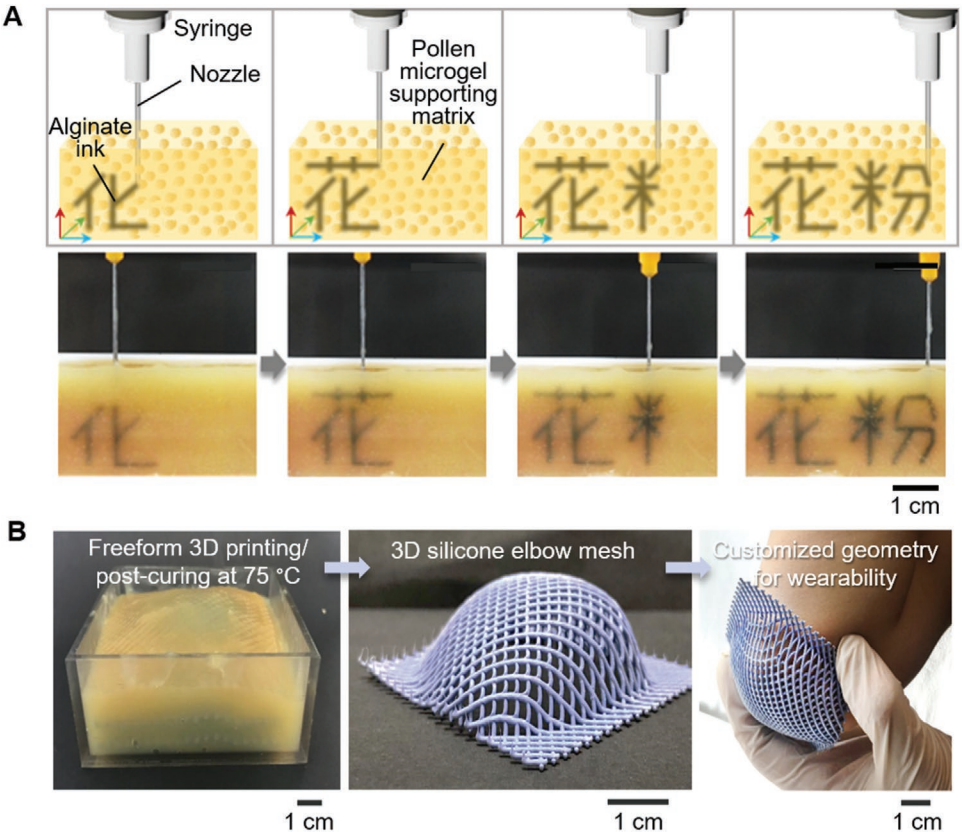

Figure 6. Freeform 3D printing of alginate hydrogel and silicone rubber inks in pollen microgel for complicated and flexible 3D architectures. A) 3D printing of Chinese characters 花粉 (meaning pollen) using alginate hydrogel ink within a pollen microgel supporting matrix. B) 3D printing of a complex 3D elbow mesh with various curvatures. Optical images of 3D printing of silicone rubber (PDMS) elbow mesh within pollen microgel after curing and fitting onto the human elbow.

A 3D elbow model was first obtained via 3D scanning from a volunteer. A 2D mesh grid was then projected to the surface of the 3D model to retrieve the coordinates. The coordinates were subjected to additional modifications to obtain the bilayer printing path for the elbow mesh. The 3D elbow mesh was omnidirectionally printed and subsequently cured in the pollen microgel-based supporting matrix. The obtained 3D silicone rubber mesh exhibited good structural fidelity, so that it could well adapt to the human elbow curvature (Figure 6B). All of the connection points were also well printed without delamination. Additionally, the mechanical properties of the silicone rubber samples printed and cured in the pollen microgel supporting matrix were similar to those of samples fabricated via the traditional casting method (Figure S11, Supporting Information). In our previous work on the alginate microgel-based supporting matrix for silicone printing, the average diameter of alginate microgels was ≈250 µm, showing a good printing quality of up to ≈1 mm resolution.[39] Since the average diameter of pollen microgels used in this work was ≈30 µm, which is an order of magnitude smaller than those alginate microgels, the printing resolution with pollen microgel was enhanced. Indeed, the printing of a smaller product size at a higher resolution was feasible with this pollen suspension, which could not be achieved with the alginate microgel-based supporting matrix (Figure S9, Supporting Information).

Notwithstanding the great potential of pollen microgels as supporting matrices for freeform 3D printing, two features should be carefully considered for real applications: the visibility of printed objects during printing and the recyclability of the microgel systems. The visibility of the pollen microgel supporting matrix was ≈2 mm from an outer surface. Thus, if the printability of simple structures using various ink materials can be demonstrated near the matrix surface, freeform 3D printing in the pollen microgel supporting matrix for real applications can be easily optimized with minimal trials. Regarding recyclability, pollen microgels have great long-term structural stability, lack significant agglomeration with adjacent microgels, and maintain their rheological properties at room temperature owing to the existence of the outer sporopollenin exine layer with spiky surface topography. Pollen microgel-based structures were thermally stable was up to 200 °C.[40] Based on our recent strategy on the recyclability of the alginate microgel-based supporting matrix,[41] the pollen suspension will be further optimized to improve recyclability under heat cycles.

3. Conclusion

In this study, we demonstrated the feasibility of a pollen-derived microgel suspension as a functional reinforcement

for composite hydrogel inks and a supporting matrix for freeform 3D printing systems. As a key component of ink materials, the pollen microgels demonstrated several remarkable advantages. The pollen–hydrogel inks were printable without jamming behavior, regardless of the pollen microgel particle content. The microgels were well dispersed within the hydrogel matrix with no significant aggregation, resulting in reproducible and uniform printed structures with good structural integrity. Moreover, the stimulus-responsive pollen microgels were used to realize functional hydrogel scaffolds with selective release. We demonstrated that the uniform and highly interconnected pores of the 3D pollen–hydrogel scaffolds could be a substitute for ICC systems for 3D cell culture applications. Furthermore, shear-thinning and viscoplastic pollen suspensions could be used as the supporting matrix for omnidirectional freeform 3D printing. Two types of inks—liquid alginate and viscoplastic silicone inks—were successfully printed, producing highly complicated 3D structures with or without a subsequent post-curing process. The pollen microgel suspension is highly advantageous as a supporting matrix because the pollen grains are an abundant and affordable starting material with a uniform size distribution and tunable rheological behavior. Finally, sunflower pollen grains were used for proof-of-concept demonstrations. Given that there are numerous types of pollen species with distinct sizes, shapes, and surface properties, pollen microgel suspensions can be used to create a new class of eco-friendly 3D printing materials.

4. Experimental Section

Materials: Defatted sunflower (*Helianthus annuus* L.) pollen was purchased from Greer Labs (USA). Silicone elastomer DOWSIL SE1700 White was purchased from DOW Corning (Japan). HAc sodium salt from *Streptococcus equi* (MW ≈ 1.5–1.8 MDa), phosphate-buffered saline (PBS), dimethylformamide (DMF), glycidyl methacrylate, tetrabutylammonium bromide, triethylamine, acetone, alginic acid sodium salt from brown algae, N-vinyl-pyrrolidinone (NVP), Irgacure 2959 (2-hydroxy-4′-(2-hydroxyethoxy)-2-methylpropiophenone), calcium chloride ($CaCl_2$), gelatin from bovine skin (type B), potassium hydroxide (KOH), mineral oil, RhB, poly(ethylene glycol) (PEG), and type 1 collagen from rat tail were purchased from Sigma-Aldrich (Singapore) and used without further purification. High-glucose Dulbecco's modified Eagle's medium (DMEM), fetal bovine serum (FBS), an antibiotic-antimycotic, L-glutamine, and sodium pyruvate were purchased from Gibco, Life Technologies. Huh-7.5 human hepatocellular carcinoma cells were obtained from Apath. A Live/Dead cell viability/cytotoxicity kit was purchased from Life Technologies.

Preparation of the Sunflower Pollen Microgel: First, 10 w/v% sunflower pollen was mixed with aqueous 10 or 30 w/v% KOH in a polytetrafluoroethylene round-bottom flask under magnetic stirring at 200 rpm. The suspension was refluxed for 2 h at 80 °C with stirring at 200 rpm and then centrifuged at 4500 rpm for 5 min. The supernatant was removed, and the sample was washed five times using fresh KOH solution with the same concentration as in the initial base-hydrolysis step. Finally, the sample was left to sit in KOH solution at 80 °C for 0, 3, 6, 9, and 12 h. Pollen with a 6 h KOH incubation time was used for the subsequent 3D printing experiments and more information about the processing details are described in past work.[20]

Preparation of RhB-Loaded Sunflower Pollen Microgel and Drug Release Study: The RhB-loaded sunflower pollen microgel was prepared as follows: first, 160 µL sunflower pollen microgel was dispersed in 0.5 mL of 1 mg mL^{-1} RhB solution mixed with 50 µL of 100 mM EDTA, and the mixture was vortexed for 5 min. The mixture was then kept at 4 °C for 20 h in the absence of light. After 20 h, 50 µL of $CaCl_2$ were added to the RhB-loaded sunflower pollen microgel suspension. The pollen microgel was separated out by centrifugation at 4500 rpm for 5 min, and then was washed with deionized (DI) water to eliminate the free RhB. A control group was prepared with the same procedure but without the RhB addition. The amounts of RhB and doxorubicin (DOX) in the system were determined by measuring absorbance at the 558-nm wavelength with an ultraviolet (UV) spectrophotometer (Boeco-S220, Germany). Then, the loading efficiency was calculated using the following equation:

$$\text{Loading efficiency}\,(\%) = \text{amount of RhB in microgel} / \text{initial amount of DOX in the system} \times 100 \quad (1)$$

First, 4 mg of DOX-loaded sunflower pollen microgel were suspended in 2 mL of DI water and incubated at 37 °C under stirring at 110 rpm in an orbital shaker incubator (LM-450D, Yihder, Taiwan). At predetermined time points, 0.4 mL of the release medium was collected, after which the medium was replenished with DI water. For the experimental group, the authors added 200 µL of 100 mM EDTA solution into the system at 25 min after the start of incubation. A control group was prepared through the same procedure but without the EDTA addition. The absorbance in the release sample was measured using a UV spectrometer (Boeco-S220, Germany) at 558 nm.

3D Printing with Pollen Microgel–Hydrogel Hybrid Inks—3D Printing with Pollen–Alginate Ink: Pollen microgel–alginate inks with pollen microgel-to-alginate ratios of 1:0, 2:1, 1:1, 1:2, and 0:1 were prepared by mixing 10 v/v% pollen microgels with 7 w/v% alginates. Using a 3DDiscovery Bench Top device (regenHU, Switzerland), the hybrid inks were printed at a feed rate of 6 mm s^{-1} under air pressures from 0.5 to 2 bar, depending on the ink viscosity. Nozzle tips with a 0.33 mm inner diameter were used for printing. For the pollen–alginate 3D scaffold, a gelatin supporting matrix was prepared using a previously proposed protocol,[15b] described as follows: Gelatin (5% w/v) was dissolved in a 0.01 M $CaCl_2$ solution at 40 °C, and then, the solution was gelled at 4 °C. Subsequently, 5 mL of the gelatin gel and 15 mL of the 0.01 M $CaCl_2$ solution were homogenized at 10 000 rpm for 1 min. The mixture was centrifuged at 4000 rpm for 2 min, and the supernatant was removed to obtain the gelatin supporting matrix. The hybrid ink with a microgel-to-alginate ratio of 1:1 was printed at a feed rate of 6 mm s^{-1} under various air pressures from 1 bar in the gelatin supporting matrix using a nozzle tip with a 0.33 mm inner diameter. Then, 0.01 M $CaCl_2$ solution was poured into the gelatin supporting matrix for the post-curing of scaffolds. The scaffolds were finally released from the supporting matrix and washed using saline solution and distilled water.

3D Printing with Pollen–HAc/Alginate Ink: UV-curable pollen microgel-HAc/alginate hybrid ink was prepared by mixing pollen microgels with GM-HAc. GM-HAc was synthesized via a previously proposed protocol:[42] HAc (1 w/v %) was dissolved in a PBS/DMF mixture with a 1:1 volume ratio. Then, triethylamine (4.4 v/v %), glycidyl methacrylate (4.4 v/v %), and tetrabutylammonium bromide (4.4 w/v %) were added in sequence. After the mixture was stirred overnight at room temperature, GM-HAc was precipitated with acetone and dissolved in distilled water to remove excess reactants. The solution was dialyzed in distilled water for 2 days, lyophilized, and stored at 4 °C.

Two types of pollen microgels were prepared for UV-curable hybrid hydrogel inks (ratio of microgel to hydrogel solution = 1:1). The normal pollen microgels were obtained from a 6 h incubation in 10 w/v% KOH solution at 80 °C. The RhB-loaded sunflower pollen gel was prepared as previously described. First, 1 mL of pollen with or without RhB was mixed with 1.5 mL of DI water. Subsequently, 80 mg of GM-HAc, 10 mg of alginate, 200 µL of NVP, and 40 mg of Irgacure 2959 were dissolved in the pollen solution to prepare the ink for 3D printing. The scaffold was then printed in the gelatin supporting matrix at a feed rate of 5 mm s^{-1} and air pressure of 3 bar using the 3DDiscovery Bench Top device (regenHU, Switzerland). The scaffold was exposed to UV light for 15 min and then removed from the supporting matrix after incubation at 37 °C for 5 min.

Freeform 3D Printing in Pollen Microgel Supporting Matrix: The pollen microgel-based supporting matrix was prepared by dispersing pollen microgels obtained from 0, 3, 6, and 9 h incubation in 10 w/v% KOH solution at 80 °C. Then, 10 vol% pollen microgels were dispersed in water, resulting in a PD of 90%. A dilution process was performed to obtain PDs of 70% and 80% for the pollen microgel-based supporting matrix. For freeform 3D printing with alginate inks, a 7 w/v% alginate solution was prepared with black food dye. The black alginate ink was directly printed in the pollen microgel supporting matrix (6 h KOH incubation, PD = 90%) without physical crosslinking at a feed rate of 6 mm s^{-1} and air pressure of 5.5 bar using the 3DDiscovery Bench Top device (regenHU, Switzerland).

For freeform 3D printing with PDMS, SE1700 inks with a white base/catalyst/mineral oil ratio of 10:1:1.5 were prepared using orange or blue food dye and then printed at a feed rate of 3–4 mm s^{-1} and air pressure of 5.5 bar. Nozzle tips with a 0.33 mm inner diameter were used for printing. The pollen microgel supporting matrix (6 h KOH incubation, PD = 90%) was prepared for freeform 3D printing. The post-curing of printed silicone rubber in the supporting matrix was conducted at 75 °C for 12 h.

Rheological Properties: The rheological properties of the pollen microgel supporting matrix and pollen–hydrogel hybrid inks were tested using a TA2000 rheometer (TA instrument, USA).

To measure the rheological properties of pollen microgel supporting matrix, a steady-state flow test was performed at shear rates from 0.1 to 200 s^{-1}. The H–B model was chosen to fit the shear stress–shear rate curve. An oscillation strain sweep test was conducted from 0.1% to 100% strain at 1 Hz. The oscillation time sweep test was performed at a frequency of 1 Hz under the following strain conditions: 1% strain for 0–5 min, 70% strain for the next 5–10 min, and 1% strain after 10 min.

The viscosity of pollen-hydrogel hybrid ink was measured using a continuous ramp test at shear rates from 1 to 100 s^{-1}.

In Vitro Cell Evaluation: 3D-printed pollen–HAc/alginate hydrogels and PEGDA ICC hydrogels, either unmodified or functionalized with type 1 collagen, an extracellular matrix protein, were used for cell studies. PEGDA was synthesized following a previously reported method,[43] and PEGDA-based ICCs were fabricated as described in a previous study.[44] A 0.2 mg mL^{-1} type 1 collagen solution in PBS was used for coating both 3D-printed pollen–HAc/alginate scaffolds and PEGDA ICCs. Huh-7.5 human hepatocellular carcinoma cells were cultured in high-glucose Dulbecco's modified Eagle's medium (DMEM) supplemented with 10% fetal bovine serum (FBS), 1% antibiotic-antimycotic, 4 mM L-glutamine, and 110 mg L^{-1} sodium pyruvate in a humidified atmosphere at 37 °C in 5% CO_2.

3D-printed pollen–HAc/alginate hybrid hydrogels and PEGDA-based ICCs were sterilized under UV light for 2 h, during which they were upturned to expose the top side to UV after 1 h. Immediately before cell seeding, each scaffold was preconditioned with 1 mL of complete culture medium for 30 min and then dried for 1 h in a humidified atmosphere at 37 °C in 5% CO_2. One million Huh-7.5 cells suspended in 25 µL of complete culture medium were seeded on the top surface of each scaffold; before the culture medium was added, the cell constructs were incubated in a humidified atmosphere at 37 °C in 5% CO_2 for 6.5 h to allow cell entrapment within the scaffold pores. The cell constructs were cultured in a humidified atmosphere at 37 °C in 5% CO_2 for up to 10 days, and the culture medium was changed every 3 days. Then, 24 h after seeding, the cell constructs were transferred to new multi-well plates. The number of seeded cells remaining in the wells unattached to the scaffolds was counted using a hemocytometer, and the cell seeding efficiency was calculated based on the results.

Cell viability was qualitatively assessed using the Live/Dead cell viability/cytotoxicity kit according to the manufacturer's protocol. Cell constructs were incubated with 4 µM calcein-acetomethoxy (calcein-AM) and 12 µM ethidium homodimer-1 (EthD-1) in complete culture medium for 1 h in a humidified atmosphere at 37 °C in 5% CO_2. An LSM 710 confocal microscope (Carl Zeiss) equipped with an Axio Observer Z1 inverted microscope (Carl Zeiss) was used to visualize the live and dead cells. ZEN software was used to obtain 3D reconstruction images. ImageJ software was used to process the Z-stack images and create sum slice projections.

Supporting Information

Supporting Information is available from the Wiley Online Library or from the author.

Acknowledgements

S.C. and Q.S. contributed equally to this work. This research was supported by Advanced Manufacturing and Engineering Individual Research Grants (AME IRG) (A1983c0031) through the Agency for Science, Technology and Research (A*STAR).

Conflict of Interest

The authors declare no conflict of interest.

Data Availability Statement

The data that support the findings of this study are available from the corresponding author upon reasonable request.

Keywords

3D printing, bioinks, bioinspired materials, biomaterials, pollen, supporting matrices, sustainability

Received: June 30, 2021
Revised: July 19, 2021
Published online:

[1] C. K. Chua, K. F. Leong, *3D Printing and Additive Manufacturing: Principles and Applications of Rapid Prototyping*, World Scientific Publishing Co., Inc., Singapore **2017**.
[2] T. D. Ngo, A. Kashani, G. Imbalzano, K. T. Q. Nguyen, D. Hui, *Composites, Part B* **2018**, *143*, 172.
[3] W. E. Frazier, *J. Mater. Eng. Perform.* **2014**, *23*, 1917.
[4] Z. Chen, Z. Li, J. Li, C. Liu, C. Lao, Y. Fu, C. Liu, Y. Li, P. Wang, Y. He, *J. Eur. Ceram. Soc.* **2019**, *39*, 661.
[5] X. Wang, M. Jiang, Z. Zhou, J. Gou, D. Hui, *Composites, Part B* **2017**, *110*, 442.
[6] a) S. V. Murphy, A. Atala, *Nat. Biotechnol.* **2014**, *32*, 773; b) C. C. Chang, E. D. Boland, S. K. Williams, J. B. Hoying, *J. Biomed. Mater. Res., Part B* **2011**, *98*, 160.
[7] a) J. A. Lewis, *Adv. Funct. Mater.* **2006**, *16*, 2193; b) R. A. Barry, R. F. Shepherd, J. N. Hanson, R. G. Nuzzo, P. Wiltzius, J. A. Lewis, *Adv. Mater.* **2009**, *21*, 2407.
[8] a) S. Utech, A. R. Boccaccini, *J. Mater. Sci.* **2016**, *51*, 271; b) A. K. Gaharwar, N. A. Peppas, A. Khademhosseini, *Biotechnol. Bioeng.* **2014**, *111*, 441.
[9] K. Kabiri, H. Omidian, M. J. Zohuriaan-Mehr, S. Doroudiani, *Polym. Compos.* **2011**, *32*, 277.
[10] a) P. Thoniyot, M. J. Tan, A. A. Karim, D. J. Young, X. J. Loh, *Adv. Sci.* **2015**, *2*, 1400010; b) T.-S. Jang, H.-D. Jung, H. M. Pan, W. T. Han, S. Chen, J. Song, *Int. J. Bioprint.* **2018**, *4*, 126.
[11] D. Chimene, R. Kaunas, A. K. Gaharwar, *Adv. Mater.* **2020**, *32*, 1902026.
[12] a) Q. Shi, K. Yu, X. Kuang, X. Mu, C. K. Dunn, M. L. Dunn, T. Wang, H. J. Qi, *Mater. Horiz.* **2017**, *4*, 598; b) Y. Jin, C. Liu, W. Chai, A. Compaan, Y. Huang, *ACS Appl. Mater. Interfaces* **2017**, *9*, 17456.
[13] a) A. S. Gladman, E. A. Matsumoto, R. G. Nuzzo, L. Mahadevan, J. A. Lewis, *Nat. Mater.* **2016**, *15*, 413; b) B. G. Compton, J. A. Lewis, *Adv. Mater.* **2014**, *26*, 5930.

[14] S. Chen, W. S. Tan, M. A. Bin Juhari, Q. Shi, X. S. Cheng, W. L. Chan, J. Song, *Biomed. Eng. Lett.* **2020**, *10*, 453.
[15] a) T. Bhattacharjee, S. M. Zehnder, K. G. Rowe, S. Jain, R. M. Nixon, W. G. Sawyer, T. E. Angelini, *Sci. Adv.* **2015**, *1*, e1500655; b) T. J. Hinton, Q. Jallerat, R. N. Palchesko, J. H. Park, M. S. Grodzicki, H.-J. Shue, M. H. Ramadan, A. R. Hudson, A. W. Feinberg, *Sci. Adv.* **2015**, *1*, e1500758.
[16] O. Jeon, Y. B. Lee, H. Jeong, S. J. Lee, D. Wells, E. Alsberg, *Mater. Horiz.* **2019**, *6*, 1625.
[17] a) T. J. Hinton, A. Hudson, K. Pusch, A. Lee, A. W. Feinberg, *ACS Biomater. Sci. Eng.* **2016**, *2*, 1781; b) W. S. Tan, M. A. B. Juhari, Q. Shi, S. Chen, D. Campolo, J. Song, *Addit. Manuf.* **2020**, *36*, 101563.
[18] A. K. Grosskopf, R. L. Truby, H. Kim, A. Perazzo, J. A. Lewis, H. A. Stone, *ACS Appl. Mater. Interfaces* **2018**, *10*, 23353.
[19] Y. Jin, A. Compaan, W. Chai, Y. Huang, *ACS Appl. Mater. Interfaces* **2017**, *9*, 20057.
[20] T. F. Fan, S. Park, Q. Shi, X. Zhang, Q. Liu, Y. Song, H. Chin, M. S. B. Ibrahim, N. Mokrzecka, Y. Yang, H. Li, J. Song, S. Suresh, N. J. Cho, *Nat. Commun.* **2020**, *11*, 1449.
[21] a) K. Fukunaga, H. Tsutsumi, H. Mihara, *Bull. Chem. Soc. Jpn.* **2018**, *92*, 391; b) C. B. Highley, K. H. Song, A. C. Daly, J. A. Burdick, *Adv. Sci. (Weinh)* **2019**, *6*, 1801076; c) S. Xin, D. Chimene, J. E. Garza, A. K. Gaharwar, D. L. Alge, *Biomater. Sci.* **2019**, *7*, 1179.
[22] a) H. Li, S. Liu, L. Lin, *Int. J. Bioprint.* **2016**, *2*, 54; b) T. Ahlfeld, G. Cidonio, D. Kilian, S. Duin, A. R. Akkineni, J. I. Dawson, S. Yang, A. Lode, R. O. C. Oreffo, M. Gelinsky, *Biofabrication* **2017**, *9*, 034103; c) J. Leppiniemi, P. Lahtinen, A. Paajanen, R. Mahlberg, S. Metsa-Kortelainen, T. Pinomaa, H. Pajari, I. Vikholm-Lundin, P. Pursula, V. P. Hytonen, *ACS Appl. Mater. Interfaces* **2017**, *9*, 21959.
[23] S. Franco, E. Buratti, B. Ruzicka, V. Nigro, N. Zoratto, P. Matricardi, E. Zaccarelli, R. Angelini, *J. Phys.: Condens. Matter* **2021**, *33*, 174004.
[24] C. Pellet, M. Cloitre, *Soft Matter* **2016**, *12*, 3710.
[25] a) J. H. Bahng, B. Yeom, Y. Wang, S. O. Tung, J. D. Hoff, N. Kotov, *Nature* **2015**, *517*, 596; b) S. Roh, A. H. Williams, R. S. Bang, S. D. Stoyanov, O. D. Velev, *Nat. Mater.* **2019**, *18*, 1315.
[26] O. Jeon, Y. Bin Lee, T. J. Hinton, A. W. Feinberg, E. Alsberg, *Mater. Today Chem.* **2019**, *12*, 61.
[27] S. Chen, T. S. Jang, H. M. Pan, H. D. Jung, M. W. Sia, S. Xie, Y. Hang, S. K. M. Chong, D. Wang, J. Song, *Int. J. Bioprint.* **2020**, *6*, 258.
[28] a) R. C. Mundargi, M. G. Potroz, S. Park, J. H. Park, H. Shirahama, J. H. Lee, J. Seo, N.-J. Cho, *Adv. Funct. Mater.* **2016**, *26*, 487; b) M. G. Potroz, R. C. Mundargi, J. J. Gillissen, E. L. Tan, S. Meker, J. H. Park, H. Jung, S. Park, D. Cho, S. I. Bang, *Adv. Funct. Mater.* **2017**, *27*, 1700270.
[29] T. Gao, H. H. Hu, P. P. Castañeda, *J. Fluid Mech.* **2011**, *687*, 209.
[30] S. A. Hamad, A. F. K. Dyab, S. D. Stoyanov, V. N. Paunov, *J. Mater. Chem.* **2011**, *21*, 18018.
[31] Y. S. Zhang, C. Zhu, Y. Xia, *Adv. Mater.* **2017**, *29*, 1701115.
[32] H. Shirahama, S. K. Kumar, W.-Y. Jeon, M. H. Kim, J. H. Lee, S. S. Ng, S. R. Tabaei, N.-J. Cho, *J. Visualized Exp.* **2016**, *114*, e54331.
[33] B. J. Bielajew, J. C. Hu, K. A. Athanasiou, *Nat. Rev. Mater.* **2020**, *5*, 730.
[34] a) T. Bhattacharjee, S. M. Zehnder, K. G. Rowe, S. Jain, R. M. Nixon, W. G. Sawyer, T. E. Angelini, *Sci. Adv.* **2015**, *1*, e1500655; b) T. J. Hinton, Q. Jallerat, R. N. Palchesko, J. H. Park, M. S. Grodzicki, H.-J. Shue, M. H. Ramadan, A. R. Hudson, A. W. Feinberg, *Sci. Adv.* **2015**, *1*, e1500758; c) M. J. Rodriguez, T. A. Dixon, E. Cohen, W. Huang, F. G. Omenetto, D. L. Kaplan, *Acta Biomater.* **2018**, *71*, 379; d) C. B. Highley, C. B. Rodell, J. A. Burdick, *Adv. Mater.* **2015**, *27*, 5075; e) T. J. Hinton, A. Hudson, K. Pusch, A. Lee, A. W. Feinberg, *ACS Biomater. Sci. Eng.* **2016**, *2*, 1781.
[35] A. K. Grosskopf, R. L. Truby, H. Kim, A. Perazzo, J. A. Lewis, H. A. Stone, *ACS Appl. Mater. Interfaces* **2018**, *10*, 23353.
[36] A. M. Compaan, K. Song, Y. Huang, *ACS Appl. Mater. Interfaces* **2019**, *11*, 5714.
[37] a) A. Blaeser, D. F. Duarte Campos, U. Puster, W. Richtering, M. M. Stevens, H. Fischer, *Adv. Healthcare Mater.* **2016**, *5*, 326; b) H. M. Pan, S. Chen, T.-S. Jang, W. T. Han, Y. Li, J. Song, *Biofabrication* **2019**, *11*, 025008.
[38] C. S. O'Bryan, T. Bhattacharjee, S. Hart, C. P. Kabb, K. D. Schulze, I. Chilakala, B. S. Sumerlin, W. G. Sawyer, T. E. Angelini, *Sci. Adv.* **2017**, *3*, e1602800.
[39] W. S. Tan, M. A. B. Juhari, Q. Shi, S. Chen, D. Campolo, J. Song, *Addit. Manuf.* **2020**, *36*, 101563.
[40] Y. Hwang, M. S. B. Ibrahim, J. Deng, J. A. Jackman, N.-J. Cho, *Adv. Funct. Mater.* **2021**, *31*, 2101091.
[41] W. S. Tan, Q. Shi, S. Chen, M. A. B. Juhari, J. Song, *Biomed. Eng. Lett.* **2020**, *10*, 517.
[42] J. B. Leach, C. E. Schmidt, *Biomaterials* **2005**, *26*, 125.
[43] D. J. Waters, K. Engberg, R. Parke-Houben, L. Hartmann, C. N. Ta, M. F. Toney, C. W. Frank, *Macromolecules* **2010**, *43*, 6861.
[44] S. S. Ng, K. Saeb-Parsy, S. J. I. Blackford, J. M. Segal, M. P. Serra, M. Horcas-Lopez, D. Y. No, S. Mastoridis, W. Jassem, C. W. Frank, N. J. Cho, H. Nakauchi, J. S. Glenn, S. T. Rashid, *Biomaterials* **2018**, *182*, 299.